

Confirmation of the Doi-Edwards Model

N. P. T. O'Connor and R. C. Ball*

Cavendish Laboratory, Madingley Road, Cambridge CB3 0HE, U.K.

Received March 16, 1992; Revised Manuscript Received June 12, 1992

ABSTRACT: We present simulation results for the Doi-Edwards model of entangled linear polymers and their stress relaxation, treating the chains as confined to Rouse-like motion within their entanglement tube. The viscosity is shown to reproduce the empirical $M^{3.4}$ law with molecular weight provided the chain ends have Rouse character to their motion, irrespective of whether chain tension or contour length fluctuation effects are included. Fourier transform methods are used to generate realizations of the endbead motions, matching earlier results obtained by real time simulations by Ketzmerick and Öttinger. Absolute agreement with experimental viscosity-molecular weight data is obtained when tube renewal effects are incorporated, using the assumption that disengaged tube acts as plasticizer. The only parameters in fitting are directly and independently measured: the plateau modulus G_N^0 and how it dilutes upon plasticization, and the (Rouse) monomeric friction factor. Tube renewal is crucial to the value of $Z_c = M_c/M_e$. Using $G(t) \propto$ (surviving tube fraction)^a, our results match experiment for $a \approx 2$, but not for $a = 1$ or 3.

Introduction

The dynamical behavior of entangled polymer melts was long the subject of various qualitatively unsuccessful theories until Edwards¹ introduced the idea that each chain is effectively confined to a tube around its coarse-grained or "primitive path", subsequently developed into a systematic theory of linear polymer rheology by Doi and Edwards. A crucial dynamical feature of the tube is that in the absence of permanent cross-links, the chain is free to move along it: this mechanism was termed reptation by de Gennes in applying the idea to chains diffusing through networks.² The original Doi-Edwards model³ envisaged that the confined chain had, in effect, all the dynamical attributes of a Rouse chain³ in one dimension. For simplicity of the rheological theory, however, the curvilinear extent of the chain was treated as fixed at the mean value associated with confinement to the tube and only the longest time (Fickian) mode of chain motion was considered: both are theoretically justified in the limit of long enough chains. A further simplifying assumption, which the present work suggests is not adequate, was that the memory of stress following, for example, a step strain was strictly proportional to the fraction of tube remaining occupied since that time:

$$\sigma(t) \propto \mu(t)$$

As the stressed tube only remains in places where the tube has been continuously occupied, $\mu(t)$ is calculated from the first-passage diffusion equation of motion of the chain ends. In the Doi-Edwards case this gives

$$\mu(t) = \frac{8}{\pi^2} \sum_{p=1, \text{ odd}}^{\infty} (1/p^2) e^{-p^2 t / \tau_d} \quad (1)$$

with τ_d the reptation time being the characteristic time for diffusion out of the tube: $\tau_d = L^2 / \pi^2 D_c$, where L is the curvilinear length of the tube and D_c is the coefficient of curvilinear diffusion of the chain along this length. An important and often neglected feature of the underlying model is that it implies

$$D_c = D_{\text{Rouse}}(M) \quad (2)$$

where the latter is the Rouse, or unentangled, diffusion coefficient extrapolated to the entangled molecular weight M in question.

The simplified Doi-Edwards theory ("simple reptation" hereafter) has had considerable success in predicting qualitatively the linear behavior and particularly quantitatively the nonlinear rheological aspects of melts of linear polymers. For the important relationship between zero shear rate viscosity η_0 and molecular weight M , it predicts a limiting power law

$$\eta_0 \propto M^3 \quad (3)$$

for melts sufficiently above the entanglement mass M_e , whereas a very wide range of experiments show a power law exponent closer to 3.4⁴ and significantly lower absolute values of η than predicted.⁵ Other predictions of the simplified Doi-Edwards theory are similarly close to experiment but with systematic departures.⁵

Various attempts have been made to include more of the full Rouse motion of the chain into the Doi-Edwards theory. Doi⁶ formulated a full treatment of the problem of first passage by the chain ends but obtained only a variational estimate of the leading correction to eq 3 for large $Z = M/M_e$: it varies as $Z^{-1/2}$ and therefore remains significant out to large molecular weights. Needs and Edwards⁷ showed that simulations fully incorporating the leading Rouse mode did not produce significant corrections, but the related "Repton" model of Rubenstein⁸ incorporating a full spectrum of such modes through a discrete model clearly does do so. More recently Des Cloizeaux⁹ introduced a time-dependent diffusion approximation to the effect of all the Rouse modes; although this does not reproduce Doi's limiting correction (see ref 10), it can by adjustment of parameters be made to fit experimental dynamical behavior. Finally Ketzmerick and Öttinger¹¹ described a real-space method of generating random time sequences having Rouse statistics and hence simulated the full Rouse motion first passage problem.

Another avenue of possible improvement on the simplest theory has been in terms of "tube renewal": the extent to which one chain's tube is relaxed due to the disengagement of others around it. It was first suggested that this effect invalidated the Doi-Edwards model altogether (see ref 12) but then was shown^{13,12} to be only a quantitative correction. Graessley¹⁴ introduced an empirical model of this effect, at the expense of an extra free parameter. An unambiguous bound on the effect is to model the disen-

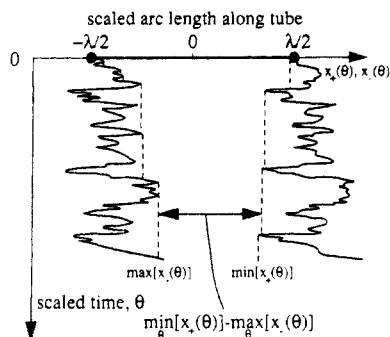


Figure 1. Fraction of original length of tube surviving, i.e., unvisited by either chain end $x_{\pm}(\theta)$ after scaled time θ .

gaged fraction as a plasticizer¹⁵ leading to $\sigma(t) \propto \mu(t)^a$ with a in the range 2–2.3; more recently Des Cloizeaux^{16,17} has suggested the “double reptation” interpretation regarding entanglements as discrete binary effects which is equivalent to $a = 2$.

In this paper we take up the original Doi–Edwards model with full Rouse mode effects, together with the plasticization model for the effects of tube renewal. Careful scaling of variables leads us to a quantitative theory of the entangled polymer viscosity *with no free parameters*, but which requires numerical simulation of its results. These we show to be in absolute agreement with experiments on a wide range of polymers.

Basic Rheological Formulation

In Rubenstein’s approximation to the full Doi–Edwards model the memory of stress after step strain is strictly proportional to the length of tube remaining continuously occupied. It therefore depends uniquely on the motion of the chain end points $X_{\pm}(t)$ along the tube arc, even when these incorporate Rouse-like motion.

Including Rouse effects, it is natural to use a rescaling of time $\theta = t/\tau_R$ in terms of the longest Rouse time

$$\tau_R = \frac{R_0^2}{3} \frac{1}{\pi^2 D_c} \quad (4)$$

and of all lengths in terms of the equilibrium end-to-end length of the coil R_0 . Then the rescaled end point motions are given by $x_{\pm}(\theta) = X_{\pm}(t)/R_0$, and the crucial parameter incorporating the degree of entanglement becomes the scaled equilibrium arc length of the tube

$$\lambda = L/R_0 = (5/4)^{1/2} (M/M_e)^{1/2} \quad (5)$$

The absolute coefficient relating this to $(M/M_e)^{1/2}$ is obtained by matching the empirical definition of the plateau modulus to the value calculated by Doi and Edwards

$$G_N^0 = k_B T c_{\text{chains}} M/M_e = {}^{4/5} k_B T c_{\text{chains}} L^2/R_0^2 \quad (6)$$

and is vital to absolute comparison below.

In terms of the end point motions we can compute (at least numerically) their maximum incursions $\min_{\theta'} [x_+(0 < \theta' < \theta)]$ and $\max_{\theta'} [x_-(0 < \theta' < \theta)]$ over a time interval of length $\theta\tau_R$, and hence the fraction of tube surviving occupied over that time (see Figure 1):

$$\mu(\lambda, \theta) = \frac{1}{\lambda} \max [0, (\min_{\theta'} [x_+(0 < \theta' < \theta)] - \max_{\theta'} [x_-(0 < \theta' < \theta)])] \quad (7)$$

Using the original Doi–Edwards formulation that stress is proportional to the remaining fraction of original tube, this gives directly the stress memory function (for step

strain) as $G(\lambda, t) = G_N^0 \mu(\lambda, t)$. Averaging over realizations and integrating with respect to time yields the (zero shear rate) viscosity:

$$\eta_0(\lambda) = \int_0^\infty G(\lambda, t) dt = G_N^0 \tau_R \int_0^\infty \bar{\mu}(\lambda, \theta) d\theta \quad (8)$$

where G_N^0 is the entanglement plateau modulus (extrapolated to infinite molecular weight). Similarly the recoverable compliance from steady-state shear flow is given by

$$J_e^0(\lambda) = \frac{\int_0^\infty t G(\lambda, t) dt}{\eta_0^2} = \frac{1}{G_N^0} \frac{\int_0^\infty \theta \bar{\mu}(\lambda, \theta) d\theta}{(\int_0^\infty \bar{\mu}(\lambda, \theta) d\theta)^2} \quad (9)$$

End Bead Dynamics and Simulation Method

The positions of the chain ends along the tube arc are given in terms of independent Rouse mode coordinates (in our scaled variables) by

$$x_+(\theta) = \frac{\lambda}{2} + \sum_{q=0}^\infty x_q(\theta)$$

$$x_-(\theta) = -\frac{\lambda}{2} + \sum_{q=0}^\infty (-1)^q x_q(\theta) \quad (10)$$

where the (scaled) Rouse coordinates $x_q(\theta)$ are independent Gaussian random processes whose statistics are defined by

$$\langle |x_0(\theta) - x_0(0)|^2 \rangle = 2d_c \theta \quad (11a)$$

and for $q \neq 0$

$$\langle x_q(\theta) x_q(\theta') \rangle = (2d_c/q^2) e^{-q^2|\theta-\theta'|} \quad (11b)$$

where $d_c = 1/3\pi^2$ is the value of the curvilinear diffusion coefficient D_c in scaled units.

The end bead motions can be cast in terms of just two independent and uncorrelated combinations of $x_q(\theta)$:

$$s(\theta) = {}^{1/2}(x_+(\theta) + x_-(\theta)) = \sum_{\text{all even } q} x_q(\theta)$$

$$\delta(\theta) = {}^{1/2}(x_+(\theta) - x_-(\theta) - \lambda) = \sum_{\text{all odd } q} x_q(\theta) \quad (12)$$

These have power spectra, obtained by substituting for the $x_q(\theta)$, Fourier transforming, and summing contributions over q , given by

$$\langle |s(w)|^2 \rangle = \frac{2d_c}{w^2} \frac{c}{2} \left(\frac{\sinh c + \sin c}{\cosh c - \cos c} \right) \quad (13a)$$

$$\langle |\delta(w)|^2 \rangle = \frac{2d_c}{w^2} \frac{c}{2} \left(\frac{\sinh c - \sin c}{\cosh c + \cos c} \right) \quad (13b)$$

$$c = \pi(w/2)^{1/2}$$

where we have normalized Fourier transforms as $f(w) = \Theta^{-1/2} \int_0^\Theta f(\theta) e^{-i w \theta} d\theta$ with Θ the length of scaled time sampled.

We have generated numerical simulations of the end point dynamics by generating Gaussian random realizations of $s(w)$ and $\delta(w)$ satisfying eq 13 and then back Fourier transforming numerically to obtain $s(\theta)$ and $\delta(\theta)$ and hence $x_{\pm}(\theta)$. The only approximation made is that the time sequence is periodic: it is important that its length Θ be kept large compared to both the Rouse time and also the overall disengagement time of the model.

Because the time sequences are only discretely rather than continuously sampled, we miss the true maximum incursions of the end points (see Figure 2). We assume

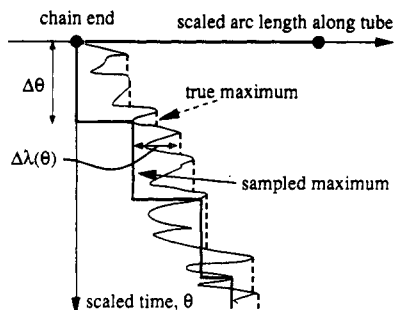


Figure 2. Difference between true and samples maximum incursions of the chain end due to sampling at discrete time points.

that it is appropriate to replace this local error by its average effect, and this can be corrected by adding to the sampled incursions

$$\Delta\lambda = b/2(\Delta\theta)^{1/4} \quad (14)$$

Here the index comes from the natural scaling of Rouse dynamics, and from studying short time sequences as a function of the sampling time step $\Delta\theta$, we find the prefactor $b = 1.1$. This agrees to within 10% with Ketzmerick and Öttinger who used different methods to generate equivalent sequences.

In all our simulations we used sequences of length $N = 2^{17} = 131\,072$ steps. Due to the scaling of $\Delta\lambda$, unrealistically high values of N would have to be used to obtain any significant reduction in $\Delta\lambda$. However, the value of θ was chosen to ensure that $2\Delta\lambda/\lambda < 0.2$ while no individual measurements spanned more than 0.125 of the total periodic time simulated. The results discussed below are based on averages of measurements of between 100 and 300 independent simulations. Because λ occurs only as an additive constant in eq 10 defining the end point motions, we reused each time sequence at several λ .

The integral (eq 8) for the viscosity η_0 can only be carried out from 0 to an upper limit of a fraction of the maximum simulation time $\nu\theta$, $\nu < 0.125$. The remaining part of the integral was evaluated by extrapolating $\bar{\mu}(\lambda, \theta)$ as a single exponential (which it will always be for $\nu\theta \gg \tau_d/\tau_R$). Provided $\bar{\mu}(\lambda, \theta)$ has decayed to a small fraction of its $\theta = 0$ value, the remainder and hence the errors involved are very small. We have used the same remainder strategy in the integrals (eq 9) for the recoverable compliance, but because of the weighting of the first moment of time θ in the numerator integral, the errors involved are larger.

One limitation of the simulations is that for sufficiently negative values of $\delta(0)$, the initial length of the chain

$$x_+(0) - x_-(0) = \lambda + 2\delta(0) \quad (15)$$

can be negative. In our simulation this gives zero stress for an entire realization as all the tube is assumed to have been vacated by the two ends passing each other. Fortunately, the probability of this occurring is less than 1% for $Z = 1$, and decreases quickly for higher Z . From the variance of $\delta(0)$ as a function of Z we could calculate the probability of having a negative start length, and then correct our value of stress. This would, however, be only an approximation as the chain potential would no longer be simply harmonic, and so this correction is not applied in this work. For the same reason it would not be valid to simply reverse the negative starting configurations.

Basic Results

Our results for $\eta_0/(G_0^N\tau_R)$ as a function of $Z = M/M_e$ are shown in Figure 3 together with those of Ketzmerick and

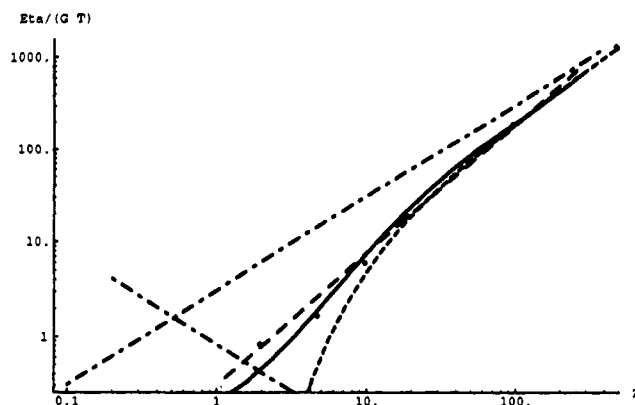


Figure 3. log-log plot of viscosity reduced as $\eta_0/G_0\tau_{Rouse}$. Simulations of reptation with full Rouse curvilinear dynamics are shown: present work (—) and data from Ketzmerick and Ottinger (---). For comparison are shown Rouse (lower) and Doi-Edwards (upper) lines (---), Doi's variational curve (---), and a line equivalent to $M^{3.4}$ (---).

Öttinger for comparison. As τ_R is proportional to M^2 , all slopes have been reduced by 2: the Rouse curve now has slope -1 and the Doi-Edwards curve $+1$. This form of plot is far more discriminating than the conventional η_0 vs M plot. It can be seen that the molecular weight exponent for η_0 is higher than 3, and for Z between 2 and 200 a straight line equivalent to $M^{3.4}$ can be drawn to fit the curve reasonably well. At high Z where the contribution from the Rouse modes becomes small, the simulation approaches the Doi-Edwards curve as a limit. Doi's variational calculation is shown for comparison.

Constant Contour Length Approximation

It should be noted that stress release only occurs at the current tail end of the chain, and the head end does not give rise to any stress loss as long as the contour length does not decrease too much. So for large Z , at any one time only the motion of one of the ends is significant, and the nature of the coupling of the two chain ends should have only a rather indirect effect on the stress release. Therefore, we have considered a chain of constant contour length, but which has the correct self-correlation for the motion of an end bead, given by

$$\langle |x(w)|^2 \rangle = s(w) + \delta(w) = \frac{2d_c}{w^2} c \left(\frac{\sinh 2c + \sin 2c}{\cosh 2c - \cos 2c} \right) \quad (16)$$

The results of simulation for constant contour length are compared with the case of correctly correlated end motions in Figure 4, and show no significant difference for $Z > 3$. We therefore conclude that it is not contour length fluctuation (cf. refs 6 and 7) as such but rather the non-Fickian motion of each chain end which causes the viscosity-molecular weight power law to be 3.4 rather than 3.

Variation in Chain Tension

Our discussion and results above have assumed the tension of the chain along the tube to be constant, whereas it follows from the original Doi-Edwards model that it should fluctuate in proportion to how stretched the chain is along the tube. Strictly speaking, for the stress memory we need to compute the degree of chain extension for only those center segments occupying the surviving tube, something which we cannot compute from the end bead dynamics alone. As an approximation which should be accurate while the stress memory is still large, we have estimated this tension on the basis of the stretch of the

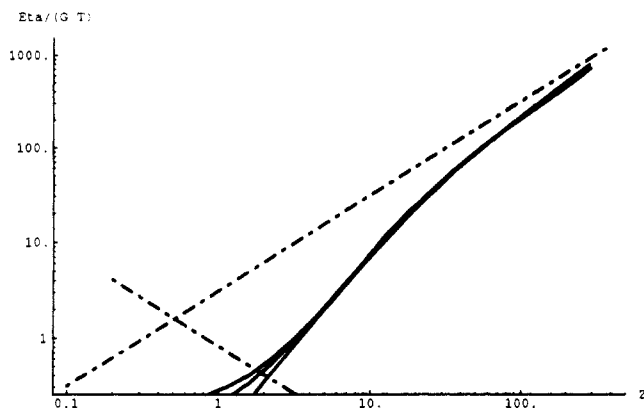


Figure 4. Comparison of various levels of model approximation, showing agreement for $Z > 3$. The solid lines represent from top to bottom (i) correct end motions with chain tension effects, (ii) correct ends without tension effects (as per Figures 3 and 4), and (iii) the constant contour length approximation (see text). Rouse and Doi-Edwards lines (---) are shown as in Figure 3.

whole chain. We then have the stress memory function including chain tension fluctuations given by

$$\mu_{\text{tension}}(\lambda, \theta) = \left(\frac{x_+(\theta) - x_-(\theta)}{\lambda} \right) \frac{1}{\lambda} \times \max [0, (\min [x_+(0 < \theta' < \theta)] - \max [x_-(0 < \theta' < \theta)])] \quad (17)$$

Note that $\bar{\mu}_{\text{tension}}$ no longer represents just the fraction of initial tube surviving, and $\bar{\mu}_{\text{tension}}(\lambda, 0)$ may differ from unity. For $Z \ll 1$ the second term dominates in eq 17, leading to $\bar{\mu}_{\text{tension}}(\lambda, 0) \approx 1/Z$ and a stress memory time of order τ_R , and hence a Rouse-like dependence on molecular weight of this contribution to the melt viscosity. However, it should be noted that the whole tube concept is suspect in this regime.

Figure 4 also shows η_0/τ_R as a function of Z with the tension effects included. At very small Z there is a crossover to pseudo-Rouse behavior, but it is negligible compared to the direct Rouse contribution which is also shown. The inclusion of chain tension does not significantly affect the value of Z_c or any of the viscosity curve for $Z > 2$, and we conclude that *chain tension fluctuations have negligible impact on the (zero shear rate) viscosity in the $\eta \approx M^{3.4}$ regime.*

Tube Renewal and Absolute Agreement with Experiment

The simplest ideas on tube renewal all lead to the ansatz that

$$G(\lambda, t) = G_N^0 \bar{\mu}(\lambda, \theta)^a$$

and hence

$$\eta_0(\lambda) = \int_0^\infty G(\lambda, t) dt = G_N^0 \tau_R \int_0^\infty \bar{\mu}(\lambda, \theta)^a d\theta \quad (18)$$

$$J_e^0(\lambda) = \frac{\int_0^\infty t G(\lambda, t) dt}{\eta_0^2} = \frac{1}{G_N^0} \frac{\int_0^\infty \theta \bar{\mu}(\lambda, \theta)^a d\theta}{(\int_0^\infty \bar{\mu}(\lambda, \theta)^a d\theta)^2} \quad (19)$$

with $a = 1$ corresponding to simple reptation and $2 < a < 2.3$ corresponding empirically to the plasticization approximation. In principle to include chain tension effects, we should take $G(\lambda, t) \approx \mu_{\text{tension}}(\lambda, \theta) \bar{\mu}(\lambda, \theta)^{a-1}$, but we will neglect this distinction in view of our conclusions above.

Figure 5 shows viscosity results from our simulations (with correctly correlated ends) for pertinent values of a .

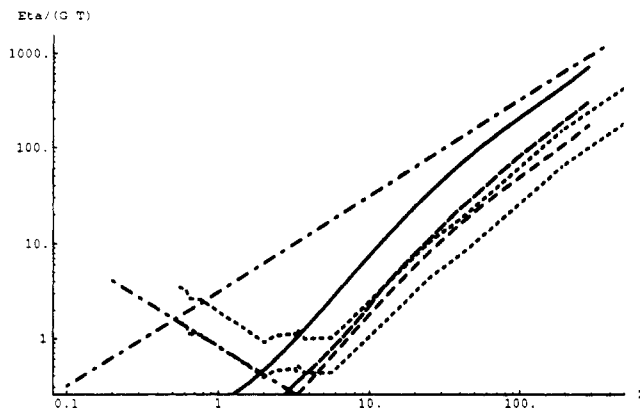


Figure 5. Effects of tube renewal and comparison with experiment for $\eta/G_0\tau_R$. Rouse and Doi-Edwards lines (---) are shown as in Figure 3; simulation results are shown for stress memory $\propto (\text{surviving tube fraction})^a$ for $a = 1$ (—), $a = 2$ (---), $a = 3$ (· · ·). Experimental data for Colby et al. are shown (···), the lower curve as reported and the upper curve scaled by Roovers' value for τ_R . The latter agrees well with $a \approx 2$ (see text).

The lowering with a is slightly more than that expected from approximating $\bar{\mu}(\lambda, \theta)$ as a single exponential decay, which predicts simply $\eta \propto a^{-1}$.

Also shown for comparison is the experimental viscosity obtained by Colby, Fetters, and Graessley (CFG)¹⁸ for polybutadiene samples over an exceptionally wide range of molecular weights. We have some doubt as to how to scale this data as CFG obtain a significantly higher monomeric friction factor ($\zeta_0 = 2.6 \times 10^7 \text{ gs}^{-1}$) than earlier work on the same material ($1.1 \times 10^7 \text{ gs}^{-1}$),¹⁹ and the Rouse times scale in proportion to this. The problem lies not with raw data, but with the differing extent to which it has been corrected for the molecular weight dependence of the glass transition temperature. Scaling using Roovers' friction factor leads to excellent absolute agreement with our calculations in the 3.4 regime corresponding to $a \approx 2$, whereas scaling by CFG's own result gives a significantly lower curve. An independent reason to consider the Roovers-based scaling seriously is that it leads to a conventional value of $M_c/M_e = 2.4$, compared to the unusually high value of 3.5 implied by scaling based on CFG (see below).

Crossover Molecular Weight Analysis

The ratio M_c/M_e of the (extrapolated) intercept M_c between entangled and Rouse viscosities to the entanglement molecular weight M_e is sensitive to the way tube renewal lowers the entangled viscosity. Indeed given that the effective 3.4 power law form is reproduced, $Z_c = M_c/M_e$ substantially quantifies the absolute agreement with experiment.

Empirically Graessley and Edwards²⁰ found $Z_c = 2.2$ in correlating M_c and M_e over 14 different polymer species. We have extracted corresponding values from our simulations. As the tube model ceases to be well-defined for small values of Z , the simulation curves for $Z < 3$ and hence the crossover point of the reptative and Rouse curves cannot be assumed to be reliable estimate of Z_c . Instead we add the Rouse viscosity as a function of Z to our simulation curves to obtain a smooth transition, and then follow experimental convention by extrapolating this with a line equivalent to $M^{3.4}$ to the point of intersection with the pure Rouse line. Our results are shown in Table I and compared to the representative value $Z_c = 2.2$ obtained by Graessley and Edwards. This provides clear experimental evidence for a tube renewal contribution (to

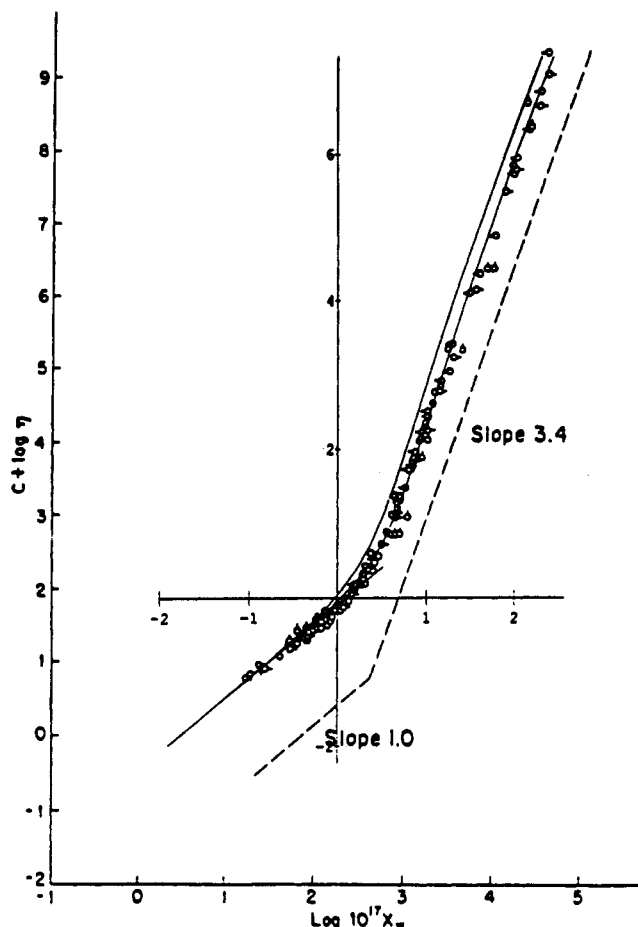


Figure 6. Comparison of theoretical viscosity with experimental data on five species due to Fox and Allen. The theoretical curves are based on simulation results without tube renewal (upper curve) and with $a = 2$ tube renewal (lower curve), with the Rouse viscosity added on. Vertical scaling is arbitrary, but horizontally we use the results of Graessley and Edwards (see text).

Table I

	$a = 1$	$a = 2$	$a = 3$	Graessley and Edwards
$Z_c = M_c/M_e$	1.6 ± 0.1	2.4 ± 0.3	2.7 ± 0.1	2.2

homopolymer viscosity) in line with double reptation ($a = 2$) or the plasticization approximation ($a \approx 2.2$).

The Doi-Edwards model with $a = 2$ tube renewal also shows absolute agreement with the viscosity-molecular weight data of Fox and Allen,²¹ as shown in Figure 6. The data (from five polymer species) were originally superposed in terms of the scaled molecular weight $X = R_g^2 \rho / m_0$, where m_0 is the mass per chain bond, which we have replotted as $Z = M/M_e = (X/X_c)(M_c/M_e)$ using Graessley and Edwards' empirical observations that data correlation over 14 species is consistent with $M_c/M_e = 2.2$ and $X_c = 1.8 \times 10^{-15} \text{ cm}^{-1}$.

Recoverable Compliance

Figure 7 shows the recoverable compliance times the plateau modulus $J_e^0 G_N^0$ as a function of Z for both $a = 1$ and $a = 2$. Simple reptation predicts a value of $6/5$ independent of Z , and the Doi-Edwards relaxation spectrum with $a = 2$ gives 1.38. Experimental values range between 2 and 3. The simulation value for $a = 1$ is approximately 1.7 for $Z < 25$, but falls toward the Doi-Edwards limit for higher Z . For $a = 2$ we see better agreement with experiment, with a value of around 2.6 at M_c' falling toward the Doi-Edwards $a = 2$ limit. These values, together with those for $\eta_{0a=2}/\eta_{0\text{Rouse}}$ (with tension

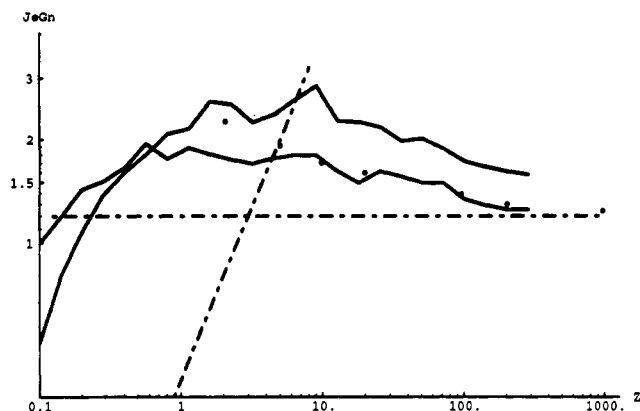


Figure 7. log-log plot of recoverable compliance time plateau modulus $J_e^0 G_N^0$ versus Z . Simulation (— and ---) and reference lines (···) are as per Figure 3.

Table II

$Z = M/M_e$	$\eta_{a=2}/\eta_{\text{Rouse}}$	$J_e^0 G_N^0 (a = 2)$
0.10	0.012	0.51
0.20	0.015	1.1
0.40	0.027	1.6
0.80	0.073	2.1
1.6	0.23	2.6
3.2	1.2	2.3
6.4	7.3	2.6
13	53	2.3
26	370	2.2
51	2.0×10^3	2.0
102	1.0×10^4	1.7
205	4.8×10^4	1.6
290	1.0×10^5	1.6

effects) are given in Table II. It should be noted however that the value of J_e^0 may be extremely sensitive to polydispersity: for $a = 1$ Needs²² suggested that it be proportional to the ninth power of the polydispersity index M_w/M_n , so we should be cautious of comparing experiment with theory in cases where the index exceeds 1.05.

Conclusions

The apparent $M^{3.4}$ power law for entangled (linear homopolymer) melt viscosity is quantitatively accounted for by Rouse fluctuation effects in the Doi-Edwards model. The crucial aspect is the time-correlated nature of the curvilinear motion of each chain end along the entanglement tube, as we have shown both contour length fluctuations and associated fluctuations in the chain tension to have negligible effect in the entangled regime.

Tube renewal effects, as modeled by double reptation or plasticization, lower fairly rigidly the entangled viscosity curve. Hence, they raise the ratio M_c/M_e of the crossover molecular weight for viscosity to the entanglement molecular weight from the plateau modulus, in good agreement with experiment.

With its Rouse effects and tube renewal added, the Doi-Edwards model is in absolute agreement with experimental viscosity measurements over several decades of molecular weight. The only scale factors involved in this comparison are material-dependent and directly measured: M_e from the plateau modulus, and the monomeric friction factor from the unentangled portion of the viscosity curve. Ambiguity as to how the friction factor has been corrected for variation in the density of chain ends is now the weakest point in our comparisons, and deserves renewed experimental attention. One strategy to get around this problem is to scale each viscosity by the corresponding coil diffusion coefficient, requiring more theory but also measurements of D and η on strictly comparable samples. The alternative

is to exploit the elegant technique of Allen and Fox,²³ studying blends of varying M_w but fixed end concentration (M_n^{-1}). To this end we are currently reappraising the theoretical implications of polydispersity.

Acknowledgment. N.P.T.O. thanks BP Chemicals Ltd. (Grangemouth) for their generous CASE award and continuous support, and also the SERC for their funding.

References and Notes

- (1) Edwards, S. F. *J. Phys. A: Gen. Phys.* **1968**, *1*, (Ser. 2), 15.
- (2) de Gennes, P. G. *J. Chem. Phys.* **1971**, *55*, 572.
- (3) Doi, M.; Edwards, S. F. *J. Chem. Soc., Faraday Trans. 2* **1978**, *74*, 1789. Doi, M.; Edwards, S. F. *The Theory of Polymer Dynamics*; Oxford University Press: Oxford, 1986.
- (4) Ferry, J. D. *Viscoelastic Properties of Polymers*; Wiley: New York, 1961.
- (5) Graessley, W. W. *J. Polym. Sci.* **1980**, *18*, 27.
- (6) Doi, M. *J. Polym. Sci., Polym. Phys. Ed.* **1983**, *21*, 667.
- (7) Needs, R. J. *Macromolecules* **1984**, *17*, 437.
- (8) Rubenstein, M. *Phys. Rev. Lett.* **1987**, *59* (17), 1946.
- (9) Des Cloizeaux, J. *Macromolecules* **1990**, *23*, 4678.
- (10) O'Connor, N. P. T. Ph.D. Thesis, University of Cambridge, 1992.
- (11) Ketzmerick, R.; Öttinger, H. C. *Continuum Mech. Thermodyn.* **1989**, *1*, 113.
- (12) Daoud, M. *J. Polym. Sci.* **1979**, *17*, 1971.
- (13) Klein, J. *Macromolecules* **1978**, *11* (5), 852.
- (14) Graessley, W. W. *Adv. Polym. Sci.* **1982**, *47*, 67.
- (15) Marrucci, G. *J. Polym. Sci. Polym. Phys. Ed.* **1985**, *23*, 159.
- (16) Des Cloizeaux, J. *Europhys. Lett.* **1988**, *5*, 437.
- (17) Des Cloizeaux, J. *Macromolecules* **1990**, *23*, 3992.
- (18) Colby, R. H.; Fetters, L. J.; Graessley, W. W. *Macromolecules* **1987**, *20*, 2226.
- (19) Roovers, J. *Polymer* **1985**, *26*, 1091.
- (20) Graessley, W. W.; Edwards, S. F. *Polymer* **1981**, *22*, 1329.
- (21) Fox, T. G.; Allen, V. R. *J. Chem. Phys.* **1964**, *41* (2), 344.
- (22) Needs, R. J. Ph.D. Thesis, University of Cambridge, 1983.
- (23) Allen, V. R.; Fox, T. G. *J. Chem. Phys.* **1964**, *41* (2), 337.